Geofísica Internacional (2001), Vol. 40, Num. 1, pp.

Depth of the Moho in northern Baja California using (P_g-P_n) travel times

Luis M. Reyes, Cecilio J. Rebollar and Raul Castro
Centro de Investigación Científica y de Educación Superior de Ensenada, (CICESE), Ensenada, Baja California, México

Received: September 4, 2000; accepted: December 13, 2000.

RESUMEN

Calculamos las profundidades del Moho a lo largo del eje del Macizo Peninsular de Baja California, usando ondas refractadas de eventos localizados en el norte de Baja California y registrados en un arreglo de 9 estaciones de banda ancha a lo largo de la latitud 31°N. Utilizamos 35 eventos localizados con RESNOM (Red Sísmica del Noroeste de México) y RANM (Red de Acelerógrafos del Noroeste de México) en el norte de Baja California. Las profundidades focales de estos eventos varían entre 3 y 15 km y las magnitudes entre 2.1 a 3.9. El modelo de velocidades en una dimensión, 1-D (Nava and Brune, 1982), fue usado para calcular los tiempos de viaje teóricos de P_g y P_n para diferentes profundidades. Las diferencias entre tiempos de viaje teóricos y observados (P_g- P_n) fueron minimizadas en un proceso iterativo a fin de encontrar la profundidad más probable del Moho a lo largo del eje del Macizo Peninsular entre las latitudes 31.3° y 31.7°N. Encontramos que la profundidad promedio del Moho es aproximadamente 42±3 km en el oeste del Macizo Peninsular, disminuyendo a 31±3 hacia el oeste a lo largo de la costa del Pacífico y 20±3 km hacia el Golfo de Baja California.

PALABRAS CLAVE: Profundidad del Moho, sismicidad, Macizo Peninsular.

ABSTRACT

Mean Moho depths along the axis of the Peninsular Ranges in northern Baja California are obtained from refracted waves of events in northern Baja California recorded on an array of 9 broadband seismic stations across the northern Baja California Peninsula at about latitude 31°N. We used 35 events located with RESNOM (Red Sísmica del Noroeste de México) and RANM (Red de Acelerógrafos del Noroeste de México) local data. Focal depths range from 3 to 15 km and magnitudes from 2.1 to 3.9. A 1-D velocity model (Nava and Brune, 1982) was used to calculate theoretical travel times of P_g and P_n for different Moho depths. The differences between observed and theoretical (P_g-P_n) travel times was minimized in an iterative process in order to find the most likely Moho depth along the axis of the Peninsular Ranges between latitudes 31.3° and 31.7°N. It was found that the average Moho depth is approximately 42±3 km in the western Peninsular Ranges, diminishing to 31±3 toward the west along the Pacific Ocean and to 20±3 km toward the Gulf of California.

KEY WORDS: Moho depth, seismicity, Peninsular ranges.

INTRODUCTION

From October 1997 to June 1998 we deployed an array of 9 broadband seismic stations along an E-W transect at about latitude 31°N, with the purpose of estimating crustal thickness and recording micro earthquakes in Northern Baja California (Figure 1). The stations recorded continuously at 40 samples per second. The array was named North Baja Transect (NBT). We used Guralp broadband seismometers, REFTEK high resolution digital stations and peripherals provided by the following institutions: Centro de Investigación Científica y de Educación Superior de Ensenada (CICESE), San Diego State University, the Southern California Earthquake Center, the University of California, San Diego and the University of Nevada, Reno. Moho depth estimates are important in order to calculate a 3-D crustal velocity model in northern Baja California and to understand the deformation of the crust in the Gulf Extensional Province.

We calculated Moho depth variations from P_g-P_n travel times using Nava and Brune's (1982) 1-D velocity model (Figure 2) and minimizing $(P_g\text{-}P_n)_{cal}\text{-}(P_g\text{-}P_n)_{obs}$ in an iterative process. We used events recorded by RESNOM and RANM networks and located with HYPO71. P_n and P_g travel times correspond to the time between the hypocenter and the NBT stations that recorded good refracted arrivals. The selected events were located along the San Miguel-Vallecitos, Sierra Juárez, and Cerro Prieto faults and recorded on the NBT array (Figure 1). Nava and Brune (1982) used refracted waves from blasts and seismic events to calculate a 1-D crustal velocity model for southern California and northern Baja California with a similar method.

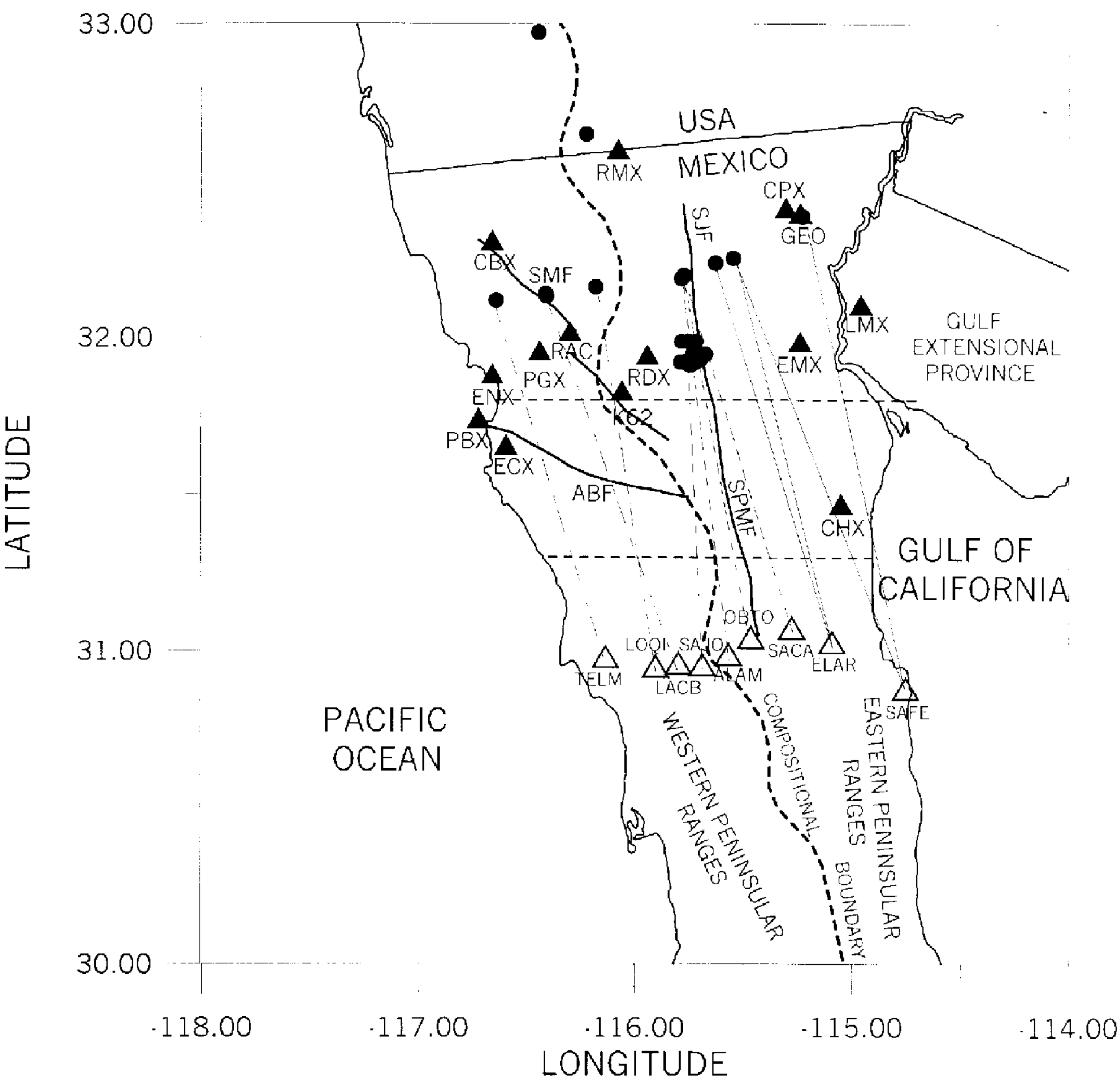

Fig. 1. Map of northern Baja California showing the locations of RESNOM and RANM stations (full triangles) as well as the North Baja Transect (NBT) broadband seismic stations (empty triangles). Northwest-southeast paths are shown by long dashed line (west batholith), short dashed lines (east batholith) and continuous lines (Gulf of California paths). Dashed horizontal line shows the area sampled by the refracted P_n phase. Continuous lines are: Sierra Juárez fault (SJF), San Miguel fault (SMF), Agua Blanca fault (ABF) and San Pedro Martir fault (SPMF).

GEOLOGICAL SETTING

The Mesozoic Peninsular Ranges batholith is divided into west and east belts separated by a magnetite-ilmenite boundary, see Figure 1 (Gastil *et al.* 1991, Silver and Chappel 1988, Baird and Miesch 1984). The western belt is 60 to 70 km wide, parallel to the Pacific Ocean. It varies from gabbros to leucogranites, with ages from 140 to 105 Ma, and is intruded by igneous rocks with ages from 125 to 118 Ma. The eastern belt ranges from tonalites to granites aged 105 to 80 Ma. (Silver and Chappel, 1988). Magistrale and Sanders (1995) and Ichinose *et al*. (1996) correlated this compositional boundary with a decreasing Moho depth from west to east. Major active faults in the Peninsular Ranges include the San Miguel-Vallecitos fault system that strikes NW-SE, the Agua Blanca fault (NWW-SEE), the Sierra Juárez fault (NNW)

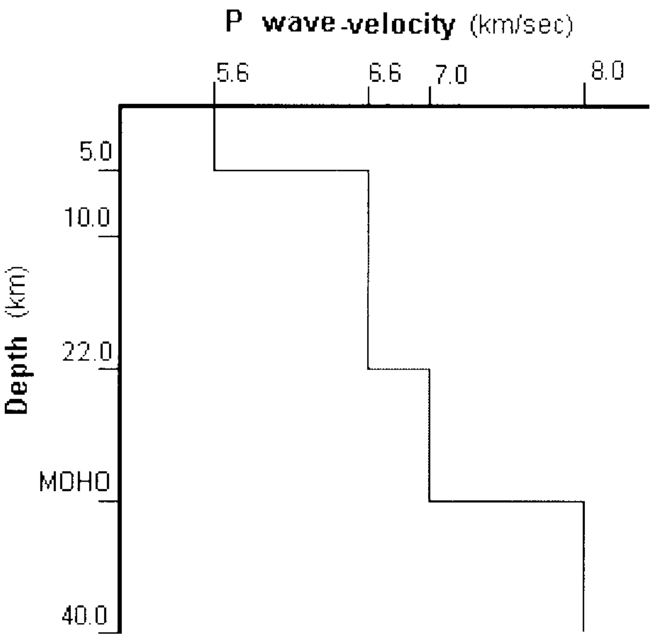

Fig. 2. One-dimensional P-wave velocity model of Nava and Brune (1982) used to calculate initial P_n and P_g travel times.

and further south the San Pedro Martir fault with a NNW trend. There is a high rate of seismic activity in this complex system of faults in the magnitude range from 2 to 4. The focal depth of the seismic activity varies from 3 to 15 km (Rebollar and Reichle, 1987).

DATA ANALYSIS

Data analysis consisted in identifying P_n and P_g phases recorded by the NBT array. Low-frequency noise was eliminated from the digital records by using a high-pass Butterworth filter with a corner frequency of 2 Hz. In some cases it was necessary to use a bandpass Butterworth filter with corner frequencies of 4 and 14 Hz in order to eliminate local high frequency noise. Figures 3-a and 3-b show examples of P_n and P_g arrival picks after filtering. Identification of P_n arrivals is straightforward and errors are of the order of ±0.05 seconds, calculated from picks from different readers. We selected 35 events with **rms** errors of less than 0.21 seconds in estimated origin time (T_0) and horizontal and depth errors from 0.5 to 2.4 km, with a magnitude range from 2.1 to 3.9 (see Table 1). Errors in the determination of T_0 will not affect the analysis, since we use (P_g-P_n) travel times.

We selected source-station paths from northwest to southeast parallel to the axis of the Peninsular Ranges in order to consider a 1-D velocity model of three horizontal layers and a half space from northwest to southeast. Magistrale and Sanders (1995) determined a 3-D velocity distribution of P waves in southern California, and found that the crust becomes more homogeneous with depth. Therefore, we developed a program to calculate travel times of P_n and P_g phases for different Moho depths using the Nava and Brune (1984) velocity model. The travel time of P_n in a 1-D velocity model of n-layers is given by

$$t = (x / V_n) + \sum_{i=1}^{n} \left(2h(d)_i / V_i\right) \cos\theta_i \,, \qquad (1)$$

where $\theta_i = \sin^{-1}(V_i / V_n)$, $h_i(d)$ is the thickness of the ith layer as a function of the hypocenter depth d, x is the epicentral distance, V_i is the P-wave velocity in the ith layer and V_n is the P-wave velocity of the upper mantle and n is the number of layers including the half space. Once the travel times were calculated, we computed $(P_g\text{-}P_n)_{cal}\text{-}(P_g\text{-}P_n)_{obs}$ and the **rms** residuals for different Moho depths. By iteration we find the minimum of the $(P_g\text{-}P_n)_{cal}\text{-}(P_g\text{-}P_n)_{obs}$ residual.

Figure 4 shows the variation of **rms** residuals for different Moho depths at stations TELM, ALAM, OBTO and SAFE. It is reasonable to expect that the error in the hypocenter will generate a large error in the Moho depth estimate. We assumed an event in the second layer of our model (depth range from 5 to 22 km) at a depth of 10 km, with a Moho depth of 20 km. The events in the Peninsular Ranges of Baja California are not deeper than 15 km (Rebollar and Reichle, 1987). Figure 5 shows a plot of Moho depth versus focal depth as a function of **rms** residuals $(P_g\text{-}P_n)_{cal}\text{-}(P_g\text{-}P_n)_{obs}$. In the iteration process we recovered a Moho depth of 20 km. However, if the hypocenters have errors of ±4 km the MOHO depth changes from 16 to 24 km. In conclusion, the maximum error is ±4 km or 20% of the Moho depth estimate (see Figure 5).

As shown in Figure 1, the refracted phases sample the Moho interface for approximately 45 km between latitudes 31.3°N and 31.7°N. We found that the crustal thickness in the Peninsular Ranges is 31±3 km at TELM station, 32±3 at LOQI, 34±3 at LACB, 36±3 at SAJO, 37±3 at ALAM, and 42±4 at OBTO. In the east, the crustal thickness is 27±3 at SACA, 21±3 at ELAR and 20±2 at SAFE. Figure 6 shows a cross section roughly between latitudes 31.3°N and 31.7°N with Moho depth estimates. Table 2 shows a summary of the results of the analysis.

CONCLUSIONS

Our crustal profile roughly follows the axis of the Penisular Ranges. At the Pacific coast the average Moho depth is 32 km; it increases gradually to a maximum depth of 42 km under Sierra San Pedro Martir and it abruptly decreases to 20 km at station SAFE on the Gulf of California. These depth estimates are averages over an area between latitudes 31.3° and 31.7°N. Our results agree with Ichinose

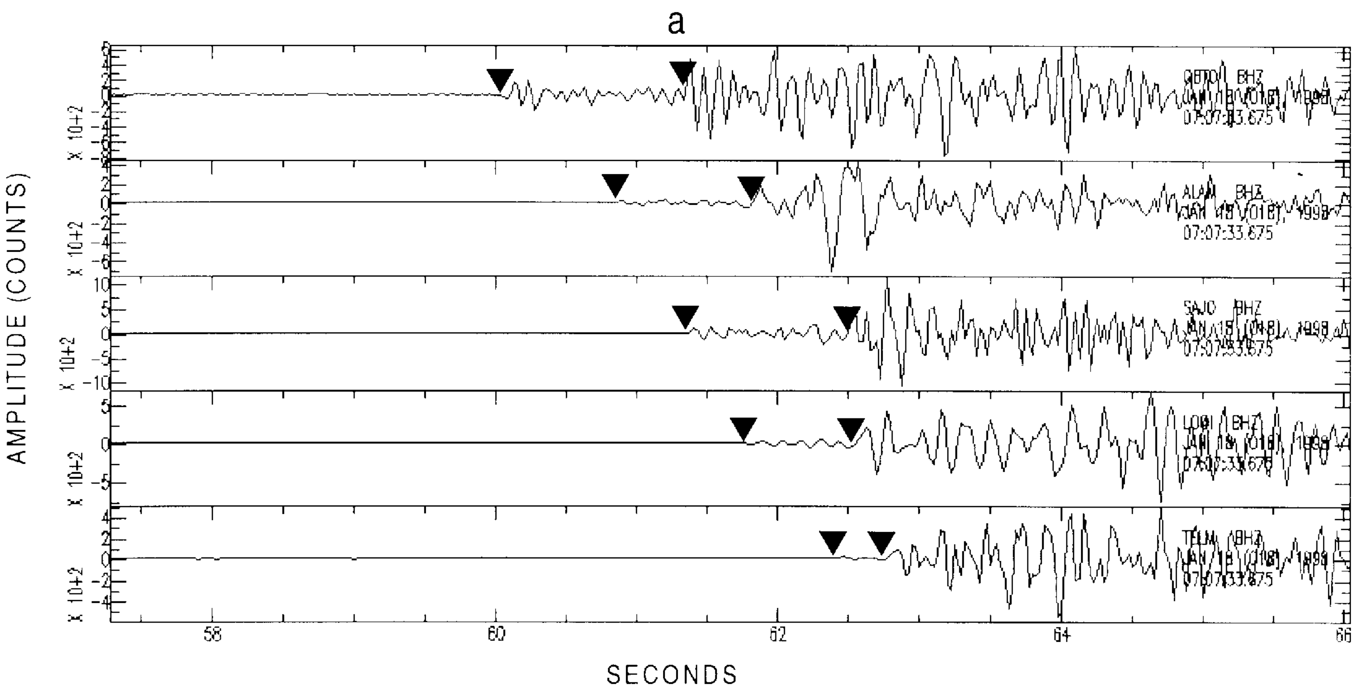

Fig. 3-a. Example of seismograms recorded by stations OBTO, ALAM, SAJO, LOQI and TELM in the Peninsular Ranges batholith. Seismograms were high-pass filtered with a butterworth filter with a corner frequency of 2 Hz. Inverted triangles indicate P_n and P_g arrivals.

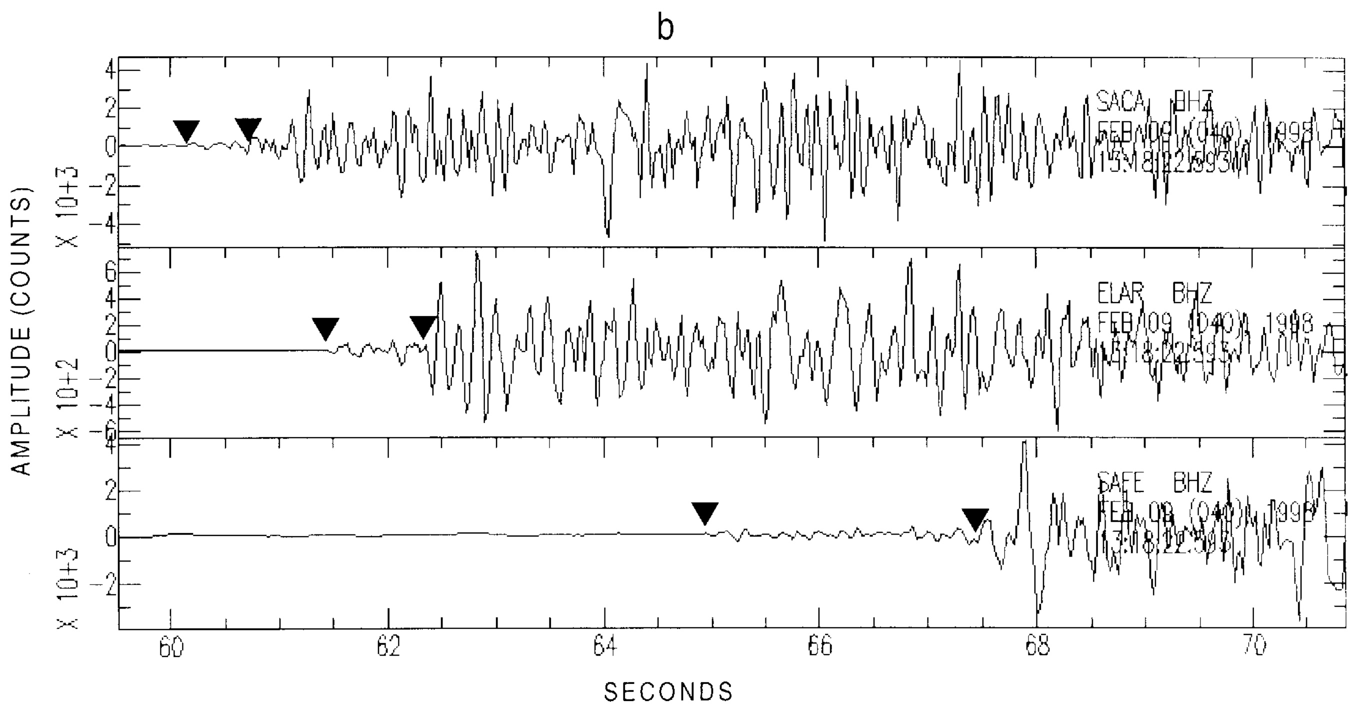

Fig. 3-b. Examples of seismograms recorded by stations SACA, ELAR and SAFE located east of the Sierra San Pedro Martir. Seismograms were high-pass filtered as above.

Table 1

Earthquakes located in northern Baja California and recorded in the NBT array

ID	DATE	ORIGEN TIME	EPICENTER		DEPTH	MAGNITUDE	RMS	DEPTH ERROR
	Y-M-D	H-M-S	LAT	LON	km	M	seconds	km
1	98-01-01	15-03-26.12	31-59.26N	115-47.06W	4.0	2.34	0.11	2.1
2	98-01-07	03-16-08.82	32-07.22N	116-38.65W	10.0	2.22	0.16	0.7
3	98-01-07	08-59-26.26	31-55.51N	115-45.02W	3.0	2.27	0.10	0.8
4	98-01-12	19-49-54.10	31-55.12N	115-45.70W	10.0	2.16	0.18	2.4
5	98-01-14	06-33-29.69	32-09.84N	116-10.97W	19.0	2.87	0.09	1.7
6	98-01-14	06-52-54.70	31-57.62N	115-43.58W	9.0	2.58	0.09	1.2
7	98-01-18	07-08-13.94	32-14.51N	115-37.79W	15.0	3.41	0.16	1.9
8	98-01-19	18-31-44.65	31-56.83N	115-40.55W	13.0	2.12	0.16	2.2
9	98-02-06	05-23-53.56	32-08.08N	116-24.67W	15.0	2.39	0.15	1.6
10	98-02-06	13-36-43.13	31-56.83N	115-42.52W	10.0	2.24	0.09	1.9
11	98-02-09	13-19-06.72	31-56.83N	115-45.22W	11.0	3.51	0.14	2.0
12	98-02-11	21-57-30.34	31-56.83N	115-43.22W	12.0	2.56	0.11	1.6
13	98-02-13	21-52-04.31	32-11.48N	115-47.15W	4.9	2.35	0.18	2.5
14	98-02-18	11-47-21.03	32-08.54N	116-24.87W	18.0	2.55	0.12	1.1
15	98-02-18	14-29-34.49	31-54.74N	115-44.75W	6.0	4.35	0.17	1.8
16	98-02-18	14-43-40.25	31-55.30N	115-43.37W	4.5	2.4	0.10	6.9
17	98-02-18	15-07-39.88	31-55.42N	115-44.06W	2.0	2.21	0.09	0.5
18	98-02-18	18-39-36.46	31-56.19N	115-44.33W	4.9	2.18	0.03	2.1
19	98-02-19	00-38-21.31	31-55.66N	115-44.22W	3.0	3.47	0.13	0.5
20	98-02-19	08-25-10.20	31-57.27N	115-43.78W	12.0	2.55	0.09	1.3
21	98-02-19	09-28-05.62	31-55.82N	115-41.92W	4.8	2.36	0.09	0.7
22	98-02-19	11-34-38.39	31-55.98N	115-42.39W	7.0	3.13	0.06	2.0
23	98-02-20	09-14-43.59	31-55.55N	115-43.02W	2.0	2.53	0.08	0.4
24	98-02-20	16-47-05.38	32-12.10N	115-46.52W	4.9	2.61	0.06	2.2
25	98-02-21	06-00-23.38	31-55.94N	115-43.93W	3.0	2.56	0.10	0.4
26	98-02-23	14-45-05.27	31-57.24N	115-43.66W	10.0	2.38	0.05	0.8
27	98-02-26	04-32-39.71	31-55.56N	115-45.56W	4.0	3.09	0.21	0.7
28	98-02-26	06-15-25.19	31-55.60N	115-44.00W	2.0	3.18	0.10	0.5
29	98-03-21	14-04-47.57	31-55.34N	115-47.40W	13.0	2.59	0.18	1.4
30	97-12-31	12-22-45.00	33.192 N	115.608 W	10.0	4.10		
31	98-01-07	07-19-12.7	32.390 N	115.230 W	4.0	3.90		
32	98-01-13	01-09-34.9	33.242 N	115.569 W	4.0	3.80		
33	98-01-20	22-11-35.56	32.256 N	115.547 W	13.0	3.10		
34	98-01-23	07-50-17.00	32.975 N	116.449 W	13.0	3.20		
35	98-01-27	00-03-29.60	32.650 N	116.226 W	11.0	3.20		

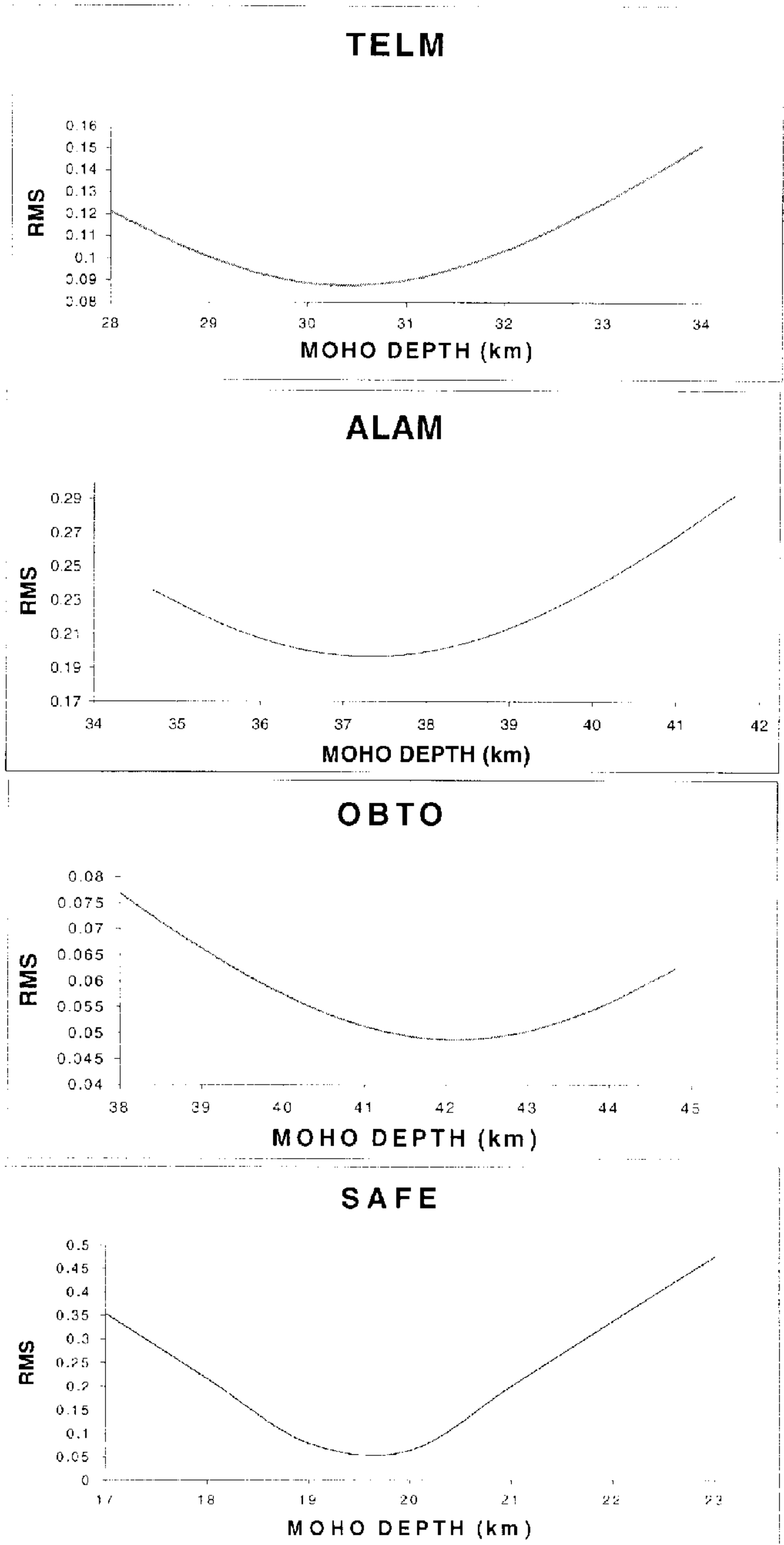

Fig. 4. Plot of the **rms** residuals versus Moho depth showing the estimate of the average crustal thickness for a path to TELM, ALAM, OBTO in the Peninsular Ranges batholith, and station SAFE in the Gulf of California.

Table 2

In this table it is shown the observed and calculated differences of P_g-P_n times, Moho depth estimates and the **rms** for each of the seismic station used

ESTACION	EVENT ID	Pg-Pn Obs.	Pg-Pn Cal.	DIFFERENCE Obs.-Cal.	MOHO DEPTH	AVERAGE DEPTH	RMS Obs.-Cal.
TELM	2	0.365	0.3271	0.0379	27.00		
	5	0.234	0.2123	0.0217	34.00		
	9	0.249	0.2562	-0.0072	30.00		
	14	0.419	0.4273	-0.0083	31.00	31	0.022517
LOQUI	2	0.205	0.2371	-0.0321	30.00		
	5	0.505	0.5013	0.0037	33.00	32	0.022848
LACB	9	0.430	0.4301	-0.0001	31.00		
	23	0.285	0.2545	0.0305	34.00		
	25	0.351	0.3858	-0.0348	34.00		
	27	0.464	0.4619	0.0021	34.00		
	28	0.454	0.3981	0.0559	32.00	33	0.032467
SAJO	1	0.328	0.3411	-0.0131	38.00		
	3	0.356	0.4134	-0.0574	34.00		
	13	1.163	1.2008	-0.0378	41.00		
	23	0.358	0.4164	-0.0584	33.00		
	24	0.523	0.5841	-0.0611	34.00		
	25	0.409	0.4169	-0.0079	34.00	36	0.044910
ALAM	5	0.364	0.3663	-0.0023	34.00		
	13	0.862	0.9294	-0.0674	41.00		
	21	0.312	0.3625	-0.0505	32.00		
	24	0.955	0.9098	0.0452	42.00	37	0.047805
OBTO	5	0.212	0.1998	0.0122	37.00		
	13	0.438	0.4378	0.0002	44.00		
	24	0.577	0.5518	0.0252	44.00	42	0.016165
SACA	7	1.569	1.5454	0.0236	24.00		
	16	1.122	1.1595	-0.0375	28.00		
	17	0.837	0.8736	-0.0366	28.00		
	19	1.157	1.1726	-0.0156	27.00		
	21	1.169	1.2135	-0.0445	26.00		
	23	1.170	1.1572	0.0128	26.00		
	27	1.114	1.1748	-0.0608	28.00		
	28	1.169	1.1865	-0.0175	26.00	27	0.034809
ELAR	7	2.056	2.0271	0.0289	21.00		
	33	2.090	2.1507	-0.0607	18.00	21	0.028900
SAFE	7	2.78	2.772	0.0080	20.00		
	30	5.443	5.3822	0.0608	17.00		
	31	2.771	2.8014	-0.0304	20.00	20	0.008000

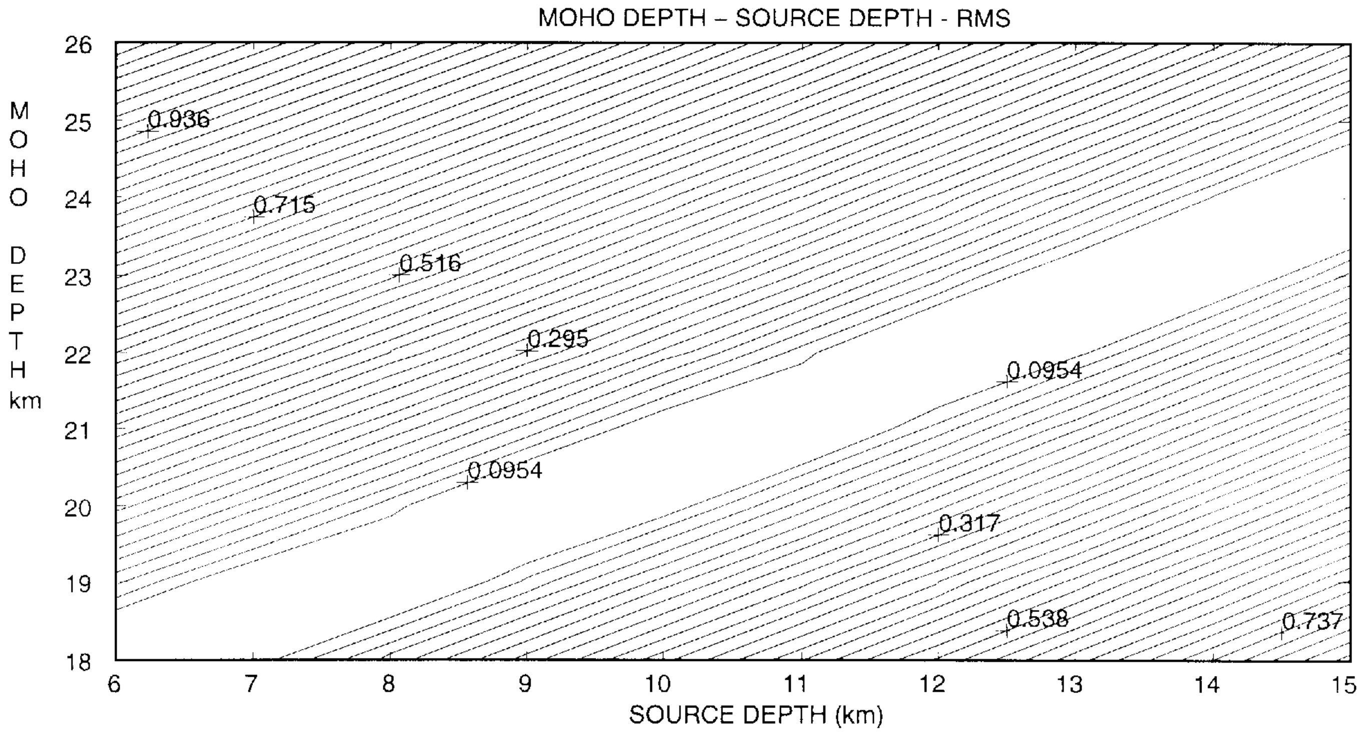

Fig. 5. Plot of the variation of the **rms** residuals as a function of Moho and focal depth. See text for explanation.

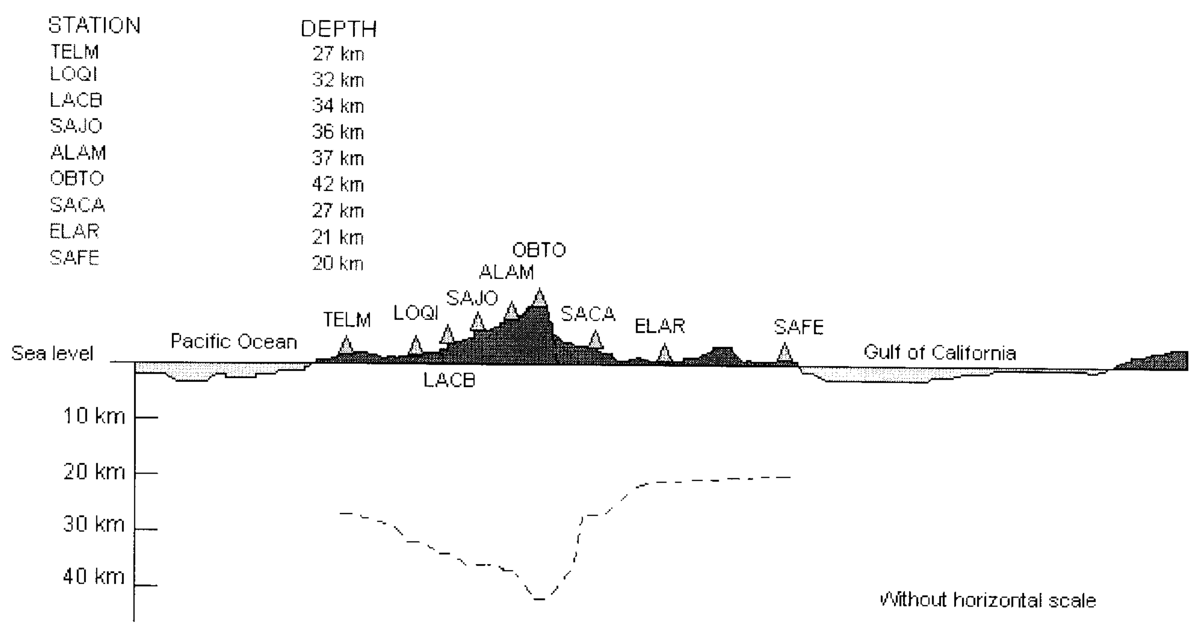

Fig. 6. Cross section of average crustal thickness in northern Baja California from the Pacific Ocean to the Gulf of California from latitude 31.3°N to 31.7°N. (Not to scale). It also shows our Moho depth estimates. Topography is indicated for reference.

et al. (1996) north of the international border, and with the estimates calculated along the NBT by Lewis *et al*. (2000). They used P-S converted phases to calculate a crustal thickness in the western Peninsular Ranges of 33 km; the crust thickened gradually toward Sierra San Pedro Martir to a depth of 43 km and decreased abruptly toward the Gulf of California to 15 km. Within errors, this crustal variation is similar to our results. Lewis *et al*. (2000) estimated Moho depths below each seismic station, using P-to-S converted phases at the crust-mantle interface. They confirmed that the topography does not correlate with Moho depth. Our method averages the Moho depth over a wide area; therefore, it is not possible to see a clear correlation between topography and crustal thickness. The thickness of the crust obtained should provide additional constraints to future 3-D velocity models for northern Baja California.

ACKNOWLEDGMENTS

We thank Arturo Pérez-Vertti, Juan A. Mendoza, Oscar Gálvez, Luis Orosco and Luis Inzunza for assistance in field maintenance of the seismic stations. Comments by Cinna Lomnitz and Luis Quintanar helped to improve the manuscript. We thank the Southern California Earthquake Center and the IRIS-PASSCAL program for loaning us some of the instrumentation used in this study. One of us (L.M.R.) is supported by a scholarship from CONACYT and SEP.

BIBLIOGRAPHY

BAIRD, A. K. and A. T. MIESCH, 1984. 1984. Batholithic rocks of southern California- a model for the petrochemical nature of their source materials. U. S. Geological Survey. Professional Paper 1284.

GASTIL, R. G., J. KIMBROUGH, Y. TAINOSHO, M. SHIMIZU and S. GUNN, 1991. Plutons of the eastern peninsular ranges, southern California, USA and Baja California, Mexico. *In:* M. J. Walawender and B. B. Hanan (eds.)"Geological excursions in southern California and Mexico, Guidebook". Geolog. Soc. of Am. SDEU annual metting, 319-131.

ICHINOSE, G., S. DAY, H. MAGISTRALE, T. PRUSH, F. VERNON and A. EDELMAN, 1996. Crustal thickness variations beneath the Peninsular Ranges, southern California. *Geophys. Res. Lett., 23,* 3095-3098.

LEWIS, J. L., S. DAY, L. ASTIZ, H. MAGISTRALE, C. J. REBOLLAR, R. CASTRO, J. N. BRUNE, J. EAKINS and F. VERNON, 2000. Regional crustal thickness variation of the Peninsular Ranges and Gulf Extensional Province, northern Baja California and southern Alta California. *Seism. Res. Lett., 71, 215.*

MAGISTRALE, H. and C. SANDERS, 1995. P wave image of the Peninsular Ranges batholith, southern California. *Geophys. Res. Lett., 22,* 2549-2552.

NAVA, F. A. and J. N. BRUNE, 1982. An earthquake-explosion reversed refraction line in the Peninsular Ranges of southern California and Baja California Norte. *Bull. Seism. Soc. Am., 63,* 1689-1698.

REBOLLAR, C. J. and M. S. REICHLE, 1987. Analysis of the seismicity detected in 1982-1984 in the northern Peninsular Ranges of Baja California. *Bull. Seism. Soc. of Am., 77,* 173-183.

SILVER, L. T. and B. W. CHAPELL, 1988. The Peninsular Ranges Bathilith: an insight into the evolution of the cordilleran batholiths of southwestern North America". *Transactions of the Royal Society of Edimburgh. Earth Sciences, 79,* 105-121.

Luis M. Reyes, Cecilio J. Rebollar and Raul Castro
Centro de Investigación Científica y de Educación Superior de Ensenada, Km 107 Carretera Tijuana-Ensenada (CICESE). 22860 Ensenada, Baja California, México